

UC Berkeley

UC Berkeley Previously Published Works

Title

Hysteresis area at the canopy level during and after a drought event in the Central Amazon

Permalink

<https://escholarship.org/uc/item/8pp319zj>

Authors

Gimenez, Bruno O

Souza, Daisy C

Higuchi, Niro

et al.

Publication Date

2024-06-01

DOI

10.1016/j.agrformet.2024.110052

Copyright Information

This work is made available under the terms of a Creative Commons Attribution-NonCommercial-NoDerivatives License, available at

<https://creativecommons.org/licenses/by-nc-nd/4.0/>

Peer reviewed

Understanding the interdependence between stomatal conductance, vapor pressure deficit and leaf water potential as water stress indicators in the Amazon

Bruno O. Gimenez, Daisy C. Souza, Niro Higuchi, Robinson I. Negrón-Juárez, Israel de Jesus Sampaio-Filho, Luiz A. Candido, Alessandro C. Araújo, Clarissa G. Fontes, Kolby J. Jardine and Jeffrey Q. Chambers

Suggested Journal: Environmental and Experimental Botany

<https://www.journals.elsevier.com/environmental-and-experimental-botany>

1. Introduction

The Amazon forest is an equilibrium system (Salati and Vose, 1984). One example is the efficient cycling of nutrients in a soil that is generally weathered and with low concentrations of phosphorus (Lugli et al., 2019), but at the same time supports a diverse and high biomass forest (Cardoso et al., 2017; Higuchi et al., 2016; ter Steege et al., 2013). This equilibrium can also be upscaled to the atmosphere layer, where in the Amazon basin it's estimated that about 50% of local precipitation is derived from the terrestrial transpiration (Chambers and Artaxo, 2017; Eltahir and Bras, 1994; Kunert et al., 2017).

At the leaf level, transpiration rate (E) is a function of vapor pressure deficit (VPD) and stomatal conductance (g_s), according to Fick's first law. The Fick's first law can be also used to

estimate the rate of net CO₂ assimilation (A_n) (Lambers et al., 2008), although there are other accurate models to estimate A_n , especially in C₃ plants (Farquhar et al., 1980). However, the Fick's first law is a simple and good approximation of E and A_n due to their inevitable connection through stomata which maximize carbon gain while minimizing water loss (Cowan and Farquhar, 1977). In normal conditions g_s varies approximately linearly with A_n , which is also an indicator of plant water use efficiency (Wu et al., 2020).

The water potential gradient regulates water movement through trees and is anchored by soil moisture availability on one end, and VPD on the other. Under non-limiting soil water availability, radiation and VPD are usually the most significant climate variables controlling water flux in tropical trees (Grossiord et al., 2019; Lloyd and Farquhar, 2008). Although the water movement in plants does not require any input of biological energy due the capillary force and the differences in water potential through the soil-plant-atmosphere continuum, the adjustable stomatal pores provides a highly effective way to avoid xylem embolism (Brodrribb et al., 2017).

In high diversity ecosystems stomata exhibit a diverse range of shapes, sizes, and numbers across plant species (Bertolino et al., 2019). In the central Amazon, some hydraulic traits are associated with topographic gradients where species from valleys (with shallow water table and high sand content) have higher efficient water transport systems compared to plateau (with deeper water table and high clay content) (Cosme et al., 2017). These species-specific signatures are probably linked to isohydric and anisohydric strategies which is associated to a higher or lower sensitivity of stomatal conductance to increases in VPD (Sampaio Filho et al., 2018). Although no consensus exists on the exact sensing mechanisms and process driving the stomatal closure response to increased VPD (Grossiord et al., 2020), the characteristics of tree species associated with adaptation to water availability (e.g., rooting depth, water storage, stomatal behavior, canopy area and leaf phenology) in high diverse ecosystems, such as Amazon forest, are critical for the improvement of current Earth System Models (ESMs) (Brodrribb et al., 2020a).

Given the importance of stomatal conductance and VPD , as respectively the mains biological and physical drivers of tree transpiration, studies focused on leaf-level measurements are extremally necessary. Previous studies showed that the relationship between transpiration (E)

and VPD is a clockwise hysteresis pattern with higher E rates during the morning period relative to the afternoon (Bretfeld et al., 2018; Brum et al., 2018; Gimenez et al., 2019; O'Brien et al., 2004). In contrast, it is possible to observe opposite patterns reflected in a counterclockwise hysteresis pattern between E and irradiance, with higher E rates during the afternoon period relative to the morning (O'Brien et al., 2004; Zeppel et al., 2004). As same as it is possible to observe diurnal differences on E rates comparing the morning and the afternoon periods, the area of hysteresis loops (H_{index}) is a good proxy for seasonal variations (Zuecco et al., 2016) and can be used as an indicator of water stress (Bretfeld et al., 2018; Brum et al., 2018).

In terms of water stress indicators, plant hydraulic characteristics are an important aspect to consider during dry conditions. Traits commonly used as indicators of water stress tolerance are the leaf water potential (Ψ_L) and stem xylem vulnerability to cavitation (Binks et al., 2016; Fontes et al., 2018). Although, some recent studies pointed that the inclusion of Ψ_L did not significantly improve prediction of g_s in tropical canopy trees (Wu et al., 2020), the use of Ψ_L in g_s models should be done by considering a more comprehensive quantification of the entire soil-plant-atmosphere continuum and pantropical transpiration sensitiveness to drought (Giardina et al., 2018; Grossiord et al., 2019; Wu et al., 2020). Isohydric species have a strong stomatal control to prevent Ψ_L from dropping below a critical threshold level (Fisher et al., 2006), and the knowledge of Ψ_L patterns, as an indicator of water stress, is extremely valuable for climate models especially in high diverse ecosystems, like the Amazon forest.

In this context, we investigated the current understanding of how stomatal conductance and VPD influences, at leaf level, the water dynamics of *terra-firme* species in the Central Amazon. To achieve this objective, an extensive data network derived from canopy level measurements using a leaf gas exchange system (LiCOR 6400XT) in the Central Amazon was used and computational simulations were performed to test the dependencies between g_s and VPD on tree transpiration according to the Fick's first law. With the observed temporal patterns of g_s and VPD , in the field, a standard H_{index} model was constructed. Additionally, computational simulations were performed contrasting the peaks, in terms of magnitude and temporal patterns, of g_s and VPD to observe their effects on transpiration patterns. Based on that we addressed two major research questions (RQ): RQ-1 What controls the hysteretic pattern of tree transpiration? RQ-2 The H_{index} (area of the loops) is a good predictor of plant water stress?

2. Materials and methods

2.1 Study area and species selection criteria

The study was conducted in an old-growth evergreen terra-firme forest located at Reserva Biológica do Cuieiras, also known as ZF-2, which contains roughly 22,000 ha adjacent to extensive areas of undisturbed tropical forest (Araújo et al., 2002) (**Figure 1**). The mean value of rainfall is $\sim 2,500$ mm year⁻¹ with the driest months of the year concentrated from July to September (Araújo et al., 2002), and with relative humidity near 90% throughout the year (Kunert et al., 2017).

In this study, the species selection was based on two distinct methods due to the difficulty to access the canopy layers in the Amazon forest. During the years of 2015-16, the species selection was based on the proximity of the tree crown's to the K-34 flux tower (02°36'33"S; 60°12'33"W). The K-34 tower have a walk-up platform which enables to access the crowns of a few species to perform leaf-level measurements (**Figure 1A**).

In addition, during the 2019 regular dry season, leaf gas exchange experiments were performed using, for the first time in the Amazon forest, a 26.0 m telescopic boom lift (Genie® Z-80/60) to access the canopy along the access road to the K-14 tower (02°35'20.570" S; 60°6'54.918"W) at ZF-2 site (**Figure 1B**). Using this equipment, it was possible to perform *in situ* leaf level measurements of many species across different canopy positions. The use of a telescopic boom lift, can be considered as a challenging in the *status quo* of ecophysiological experiments in the Amazon forest since most of surveys were conducted using towers, climbing techniques or/and canopy access walkways.

Mixing these two types of approach it was possible to perform leaf-level measurements in 30 species distributed in XX botanical families and in different canopy positions. The species, the method to access the crown and the sensors used in each species can be visualized at **Supp. Table1**.

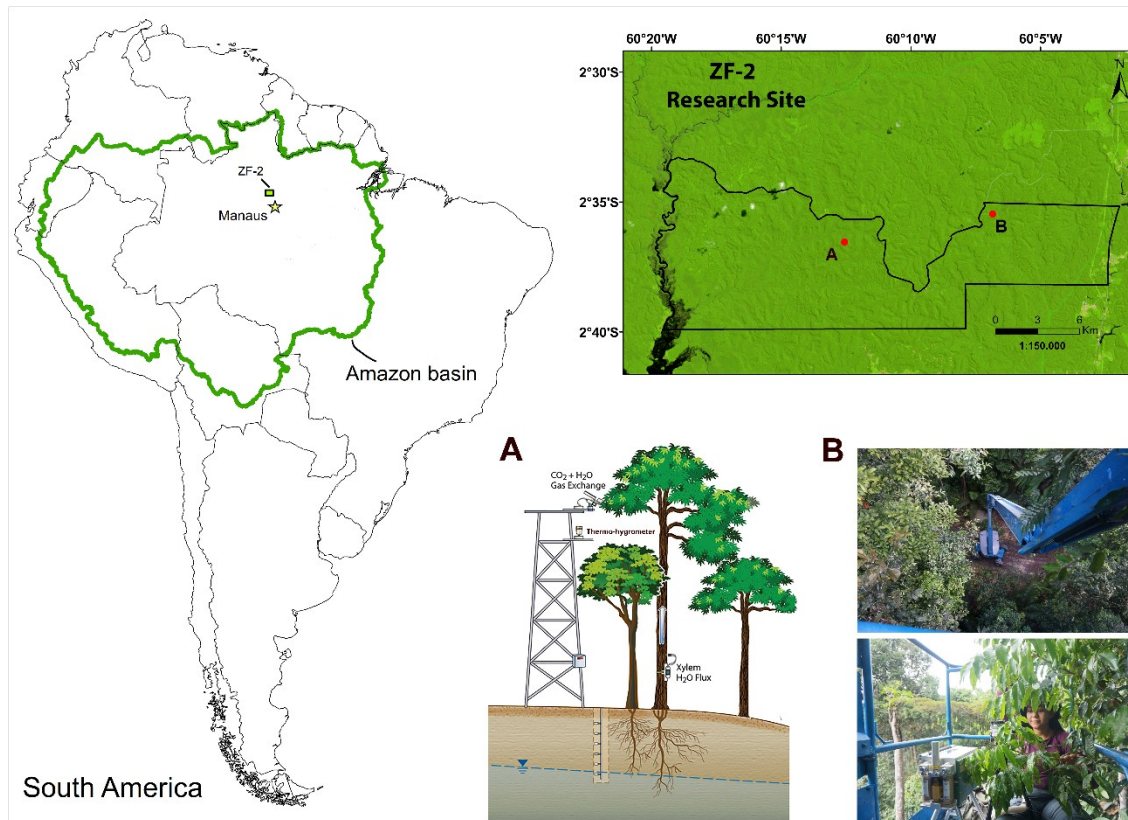


Figure 1 - Map of Amazon basin with the location of ZF-2 site near the city of Manaus, in the Central Amazon. In the upper left panel are shown the ZF-2 site limits developed using Landsat 8 satellite images (available in <https://earthexplorer.usgs.gov/>). The red dot (A) is the K-34 flux tower and the red dot (B) is the access road to K-14 tower where the telescopic boom lift (Genie® Z-80/60) was used. In both areas leaf-level measurements were performed using different species along different canopy levels.

2.2. Stomatal conductance (g_s) measurements

2.2.1 Diurnal patterns of g_s in upper canopy leaves accessed by K-34 tower

In this study, the crowns of the species *Pouteria anomala* and *Eschweilera cyathiformis* were accessed using the K-34 tower structure (**Figure 1A**). Diurnal leaf-level measurements were performed at 10-min intervals during all over the day (6:00 to 18:00) using a portable leaf gas exchange system (LiCOR 6400XT®, Lincoln, NE, United States) with a clear top chamber allowing for natural variation in PAR levels during the sampling period of randomly selected

days in the years of 2015 and 2016. The CO₂ reference concentration was held constant at 400 μmol mol⁻¹ and the T_{block} was set to achieve a target T_{leaf}, based on the observations of infrared radiometers sensors (IRR - SI-111 Apogee®) installed in the tower structure and with the target view to sun-exposed leaves of *P. anomala* and *E. cyathiformis*.

2.2.2 Canopy survey of g_s patterns using a telescopic boom lift

In addition to the leaf-level measurements of *P. anomala* and *E. cyathiformis* at the K-34 tower, leaf gas exchange experiments were performed during the 2019 regular dry season along the 500 m access road to the K-14 tower, at ZF-2 site (~20 km of distance from K-34 tower - **Figure 1B**). The equipment used to access the canopy was a 26.0 m telescopic boom lift (Genie® Z80/60). Rapid g_s measurements were done on sun-exposed leaves during approximately 10 minutes per leaf (until the g_s patterns get constant) of different species (**Supp. Table 1**). The CO₂ reference concentration was held constant at 400 μmol mol⁻¹, as same as T_{block} at 31°C to achieve a target T_{leaf} and irradiance at 1,000 μmol quanta m⁻² s⁻¹. The value of 31°C was based on the optimum temperatures for photosynthesis (T_{Opt}) already observed for tropical tree species (Slot and Winter, 2017).

2.3. Vapor pressure deficit (VPD) measurements

In this study, air temperature (T_{air}) and relative humidity (R_H) data were obtained using a thermohygrometer (HC2S3, Campbell Scientific, Logan, UT, USA) installed above the canopy at 51.1 m height in the K-34 tower structure. T_{air} and R_H were measured every 60 s and recorded as 30 min averages during 2015 and 2016. VPD was calculated using the Clausius-Clapeyron equation. All this dataset was provided by the Large-Scale Biosphere-Atmosphere Program (LBA) at the National Institute of Amazonian Research (INPA).

2.4. Leaf-level transpiration rates (E) and sap flow rate

According to the Fick's first law the leaf conductance for net CO₂ assimilation (A_n) can be derived for leaf transpiration (E) through the following equations 1 and 2 (Lambers et al., 2008). The main factors that controls E can be expressed by the resistances to water vapor diffusion along the vapor pressure gradient between leaf and atmosphere and the stomatal conductance as demonstrated by the followed equation (Woo et al., 1966).

$$E = g_s * (\omega_i - \omega_a) \quad (1)$$

Where: E is the transpiration rate in mol m⁻² s⁻¹; g_s is the stomatal conductance in mol m⁻² s⁻¹; ω_i and ω_a are the mole or volume fractions of water vapor in the air in the intercellular spaces and in air, respectively.

It is possible to derive the equation 1 into the equation 2, where ω_i and ω_a can be expressed as a result of evaporative demand (VPD) as follows:

$$E = g_s * \left(\frac{VPD}{BP} \right) \quad (2)$$

Where: E is the transpiration rate in mol m⁻² s⁻¹; VPD is the vapor pressure deficit in kPa; BP is the barometric pressure in kPa (101.3 – sea level); g_s is the stomatal conductance in mol m⁻² s⁻¹

In order to intercompare the leaf-level transpiration rates (E) with stand sap flow rates in diurnal time scales (06:00 to 18:00), sap velocity sensors were installed in two trees (*P. anomala* and *E. cyathiformis*), which were the only two species with their leaves accessible to perform leaf-level *in situ* measurements during the year of 2015. One heat pulse sap velocity sensor (SFM1, ICT international®) was installed per tree near the diameter at breast height (DBH) following the quality assessment and quality control (QA/QC) protocols described by (Christianson et al., 2017). The SFM1 sensor consists of a heater and two temperature-sensing probes to determine sap velocity (cm h⁻¹) at 0.75 cm (outer) and 2.25 cm (inner) depths in the stem using the heat ratio method (Burgess et al., 2001; Green et al., 2003) (Equation 3). The heater needle was

configured to emit a 20 Joule pulse of thermal energy every fifteen minutes (sap heat ratio measurements for 5 min 32 s following the pulse).

$$V_s = \frac{k}{x} \ln\left(\frac{v_1}{v_2}\right) * 3600 \text{ cm h}^{-1} \quad (3)$$

Where: k is the thermal diffusivity of wet wood; x is the distance between the heat source (heater) and temperature sensors; v_1 and v_2 are the increases in temperature (from ambient) at equidistant points downstream and upstream from the heater

To determine the sap flow rate, the sapwood area (A_s) was estimated using the equation developed by (Aparecido et al., 2019), which adjusted A_s as a function of diameter at breast height (DBH) using 34 trees belonging to 26 species in the same study area (ZF-2). In ZF-2 site, DBH has a moderate and non-linearly relationship with A_s ($A_s = 0.823 \times \text{DBH}^{1.781}$, $R^2=0.46$, $p<0.001$) as observed by (Aparecido et al., 2019). Using the equation from Aparecido et al., 2019 the estimated sapwood area for the species *E. cyathiformis* was 5.47 cm² and 12.23 cm² for the species *P. anomala*. Biophysical characteristics (DBH and bark thickness) for each tree can be visualized in Table 1 and were used as input into the Sap Flow Tool version 1.4.1 (Phyto-IT[®]) to calculate the sap flow rate (cm³ h⁻¹). The sap flow rate (SF) was obtained by the product between the sap velocity (V_s) and the sapwood area (A_s) ($SF = A_s \times V_s$). A linearly decrease of sap velocity was considered from the outer thermistor (0.75 cm) to the inner thermistor (2.25 cm), such that it reaches 0 at the estimated heartwood boundary. For all those estimative, a standard value of thermal diffusivity of wood (0.0025 cm² s⁻¹), sapwood fresh weight (1 g) and sapwood dry weight (0.5 g) was adopted.

2.6. Leaf water potential (Ψ_L) and canopy surface temperature (T_{canopy}) measurements

Hourly Ψ_L (6:00 to 18:00 – 12 hours) was measured using a Scholander pressure chamber (PMS, Corvallis, OR, USA; accurate to 0.05 MPa). The species selection criteria were based on the proximity of the crowns to the K-34 tower. Measurements of healthy leaves, without

noticeable condensation on the surface, were made as soon as the leaf was cut from the branch of the species *Eschweilera cyathiformis* (S.A.Mori) (Lecythidaceae) with 14.3 cm of DBH and 19.8 m in height, *Eschweilera* sp. (Mart. ex DC.) (Lecythidaceae) with 29.7 cm of DBH and 27.8 m in height, *Pouteria anomala* ((Pires) T.D.Penn.) (Sapotaceae) with 35.3 cm of DBH and 31 m in height, *Couepia longipendula* (Pilg.) (Chrysobalanaceae) with 28.1 cm of DBH and 23.9 m in height and *Pouteria erythrochrysa* (T.D.Penn) (Sapotaceae) with 36.5 cm of DBH and 29.3 m in height. In total, two years (July 2015 to August 2017) of diurnal leaf water potential experiments were conducted at ZF-2 site, as the longest record in the Amazon forest to date.

To measure canopy surface temperature (T_{canopy}) five infrared radiometer sensors (SI-111 and SI-131, Apogee®; accuracy of ± 0.2 °C) were positioned from the K-34 tower structure with the field of view targeting the top of individual tree crowns.

Five-min averages of T_{leaf} were recorded using a CR-3000 (Campbell Scientific® for the SI-111 sensors) and EM-50 (Decagon® for the SI-131 sensors) dataloggers. The sensors were positioned with the viewing heights and viewing angles listed in Table 1.

The SI-111 sensors were configured to scan leaf temperatures every 5 s and record five-min averages using a CR-3000 datalogger (Campbell Scientific®). The field of view of each sensor (T_{leaf} target area) was calculated using the IRR calculator available in the website (<https://www.apogeeinstruments.com/irr-calculators/>).

2.5. Data analysis

Data were analyzed using IGOR Pro® version 8.0 (WaveMetrics, Inc. USA) and R v. 3.0.2 (R Development Core Team, 2013) software's. For the normalization of each variable the min-max feature scaling method was used to standardize the range of the raw data of g_s and VPD . Hysteresis indices of transpiration (E) were calculated using the shoelace formula (Braden, 1986) (Equation 5), and a paired t -test was performed ($\alpha = 0.05$) to intercompare the H_{index} of the species between the 2015 and 2017 dry seasons. The H_{index} is a measure of the size of the

hysteresis loop and enables quantitative comparisons of hysteresis behaviors during, for example, two contrasting periods like El Niño and regular season.

$$H_{index} = \frac{1}{2} \sum_i \dots \quad (4)$$

Where: A is the area of the polygon, n is the number of sides of the polygon, and (x_i, y_i) , $i = 1, 2, \dots, n$ are the vertices (or "corners") of the polygon.

Results

(RQ-1) The interdependence between stomatal conductance and vapor pressure deficit on leaf-level transpiration rates (*E*)

In this study, the average of *VPD* daily patterns revealed a sensitive increase during the morning period reaching a peak in the early afternoon (14:00 – Local Time; average 0.56 ± 0.53 kPa), (**Figure 2A, B**). In contrast, stomatal conductance (g_s) daily patterns showed higher increases in the early morning peaking at 10:00 – Local Time (average 0.14 ± 0.10 mol m⁻² s⁻¹) with an expressive decrease along the afternoon period (**Figure 2A, B**). In average, the temporal difference between the peaks of *VPD* and g_s in the Central Amazon was four hours.

In addition, clockwise hysteresis pattern was observed between *E-VPD* with morning period showing higher *E* sensitivities than afternoon, due to stomatal effect (g_s effect) (**Figure 2C**). In contrast, counterclockwise hysteresis pattern was observed between *E* and g_s (**Figure 2D**), with higher *E* rates in the afternoon relative to the morning period due to *VPD* effect. The leaf-level transpiration (*E*) was represented in absolute units and calculated according to Fick's first law (**Equation 2**). The observed hysteresis patterns were a result of the temporal difference between the peaks of *VPD* and g_s , as demonstrated in **Figure 2A, B**. The calculated H_{index} for *E-VPD* was 0.224. The calculated H_{index} for *E- g_s* was 0.174, a difference of 22.3% in comparison to

the H_{index} of E - VPD . Both calculated H_{index} represents the average of VPD values from 2015-16 years and diurnal patterns of g_s of 30 species during the years 2015, 2016 and 2019.

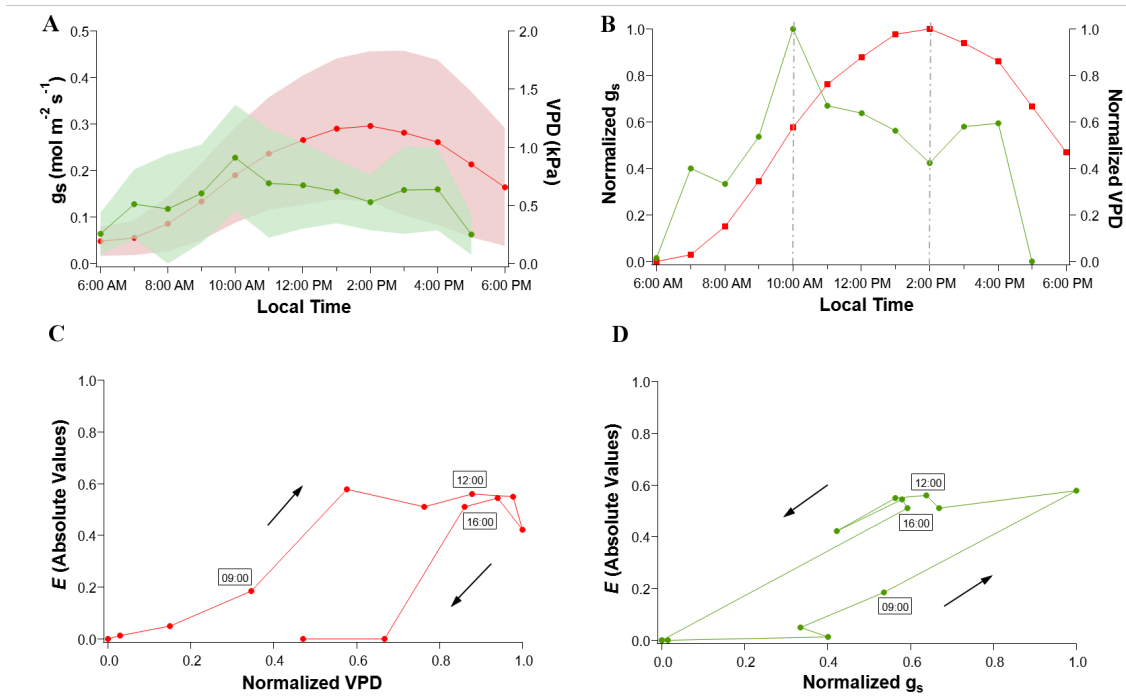


Figure 2 - Average of stomatal conductance (g_s) and vapor pressure deficit (VPD) daily patterns in the central Amazon. The observed VPD peak (red line) was at 14:00 Local Time, using hourly averages data from 2015-16 at K-34 tower (**A**, **B**). The observed g_s peak (green line) from hourly leaf gas exchange data of 30 species was at 10:00 Local Time (**A**, **B**). Clockwise hysteresis pattern was observed between E - VPD with morning periods showing higher E sensitivities than afternoon (**C**). In addition, counterclockwise hysteresis pattern was observed between E - g_s (**D**), with higher observed E rates in the afternoon relative to the morning period.

(RQ-2) The H_{index} is a good predictor of plant water stress?

Computational simulations were performed to contrast temporal (TA_x) and spatial (NA_y) amplitudes of g_s and VPD , using hypothetical values (ranging from 0 to 1), to posteriorly test their influences on transpiration patterns according to Fick's first law (**equation 2**). When the peak of g_s and VPD matches temporally ($NA_y=0$), the relationship between transpiration (E) and VPD (E - VPD) follows an exponential pattern ($y=y_o+Ax^{pow}$) (**Figure 3A**), as same as the relationship between transpiration and stomatal conductance (E - g_s). In scenario 1, it is possible to

observe that the adjusted power functions for each scatterplot (E - VPD and E - g_s) showed the same statistical values (e.g., exponent parameter (pow) $2 \pm 2.05e-09$) (**Figure 3A**). As the peaks of g_s and VPD no longer coincide temporally, the phenomenon of hysteresis emerges (**Figure 3B, C, D**). The hysteresis patterns between E - VPD and E - g_s are linked to the temporal differences between the peaks of g_s and VPD . The greater TA_x , the greater will be the H_{index} (**Figure 3B, C, D**). As TA_x increases in the different scenarios, the H_{index} values of E - VPD increased in a rate of 67% (scenario 2 \rightarrow scenario 3) to 14% (scenario 3 \rightarrow scenario 4). The area of loops (H_{index}) of E - VPD started from zero in Scenario 1 ($TA_x=0$, exponential pattern), to 0.18 (Scenario 2), 0.31 (Scenario 3) and finally 0.36 (Scenario 4). The H_{index} values of E - g_s increased in in a rate of 83% (scenario 2 \rightarrow scenario 3) to 4% (scenario 3 \rightarrow scenario 4). The H_{index} of E - g_s also started from zero in Scenario 1 ($TA_x=0$, exponential pattern), to 0.17 (Scenario 2), 0.31 (Scenario 3) and finally 0.32 (Scenario 4). No significant differences were observed between the H_{index} of E - g_s and the H_{index} of E - VPD across the different scenarios ($p=0.16$, $\alpha=0.05$, paired t -test).

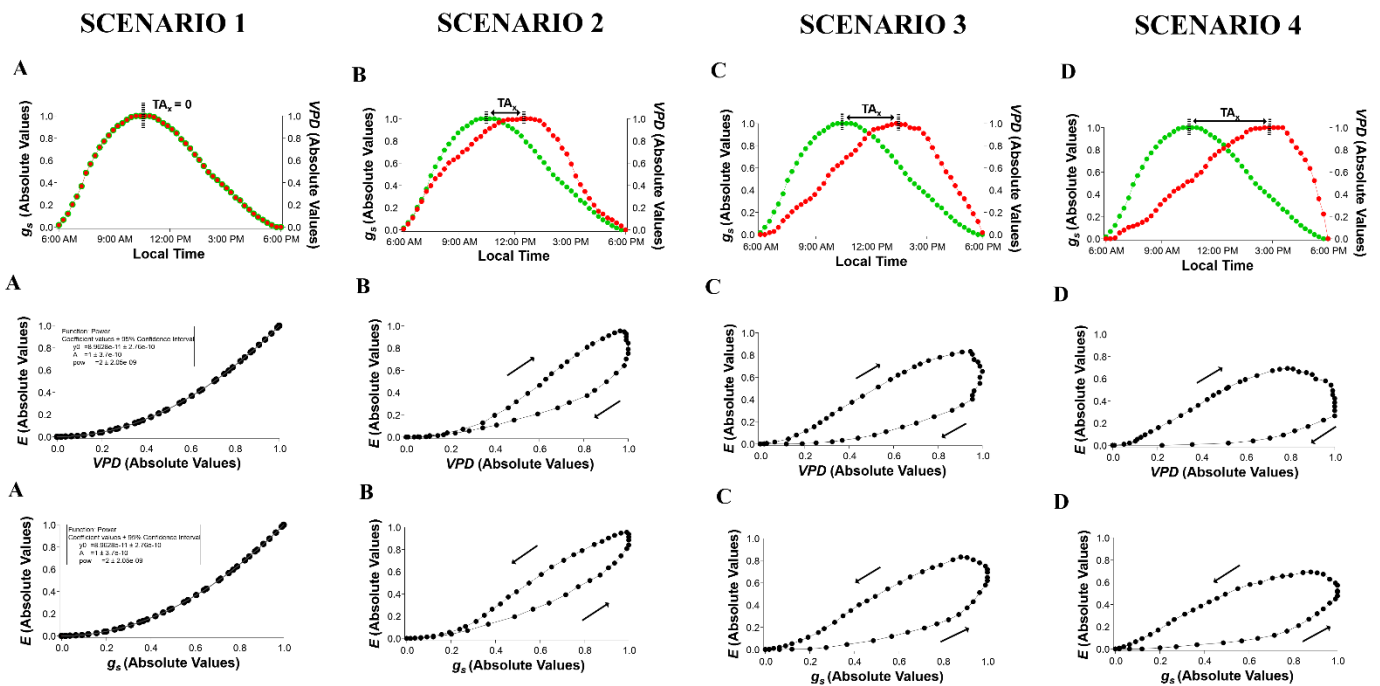


Figure 3 – Computational simulations of hysteresis phenomena in transpiration (E), testing different scenarios along temporal amplitudes (TA_x) between the peaks of g_s and VPD . In the absence of temporal difference ($TA_x=0$), no hysteretic patterns were observed between E - VPD and E - g_s , where the relationship follows an exponential pattern (A). The greater TA_x , the greater will be the H_{index} (B, C, D).

g_s values were halved in comparison to VPD values in order to test additional effects of a numerical amplitude (NA_y) on H_{index} simulating a possible drought induced effect where plants close their stomata to avoid excessive water loss. With this type of approach, it was possible to test the effects of NA_y on H_{index} . When g_s and VPD patterns matches temporally but not spatially ($TA_x=0$; $NA_y \neq 0$), the relationship between E - VPD and E - g_s still follows an exponential pattern

(**Figure 4A**), similar to when g_s and VPD patterns matches both temporally and spatially ($TA_x=0$; $NA_y=0$) (**Figure 3A**). However, although the statistical values are different in terms of the exponential parameter (pow) and the scaling factor (A).

The simulations contrasting the numerical amplitude (NA_y) between g_s and VPD in combination with the temporal amplitude (TA_x) on

The numerical amplitude (NA_y) between g_s and VPD has no effect in the shape of hysteresis phenomenon of transpiration (clockwise or counterclockwise) (**Figure 4B, C, D**) o in the transpiration of tropical trees. The generated hysteresis did not change their area, shape or slope when only the VPD values were doubled. The isolated effect of increased VPD had no effect on the hourly hysteresis phenomenon between V_s and VPD .

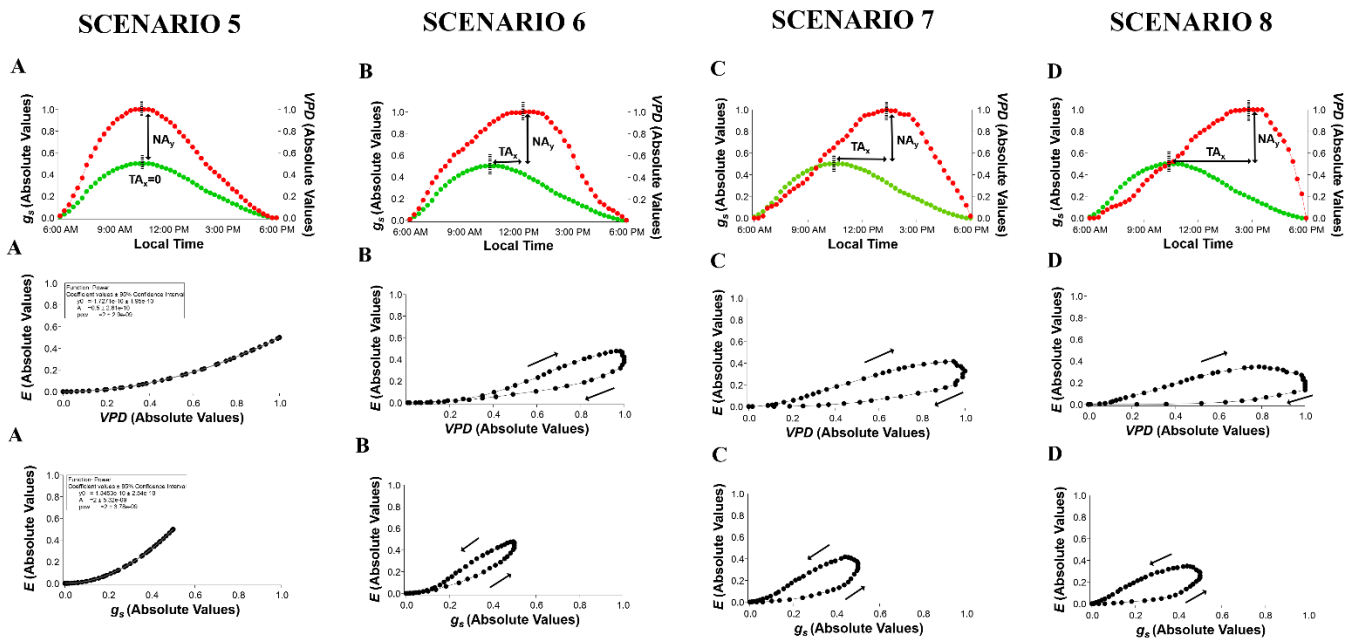
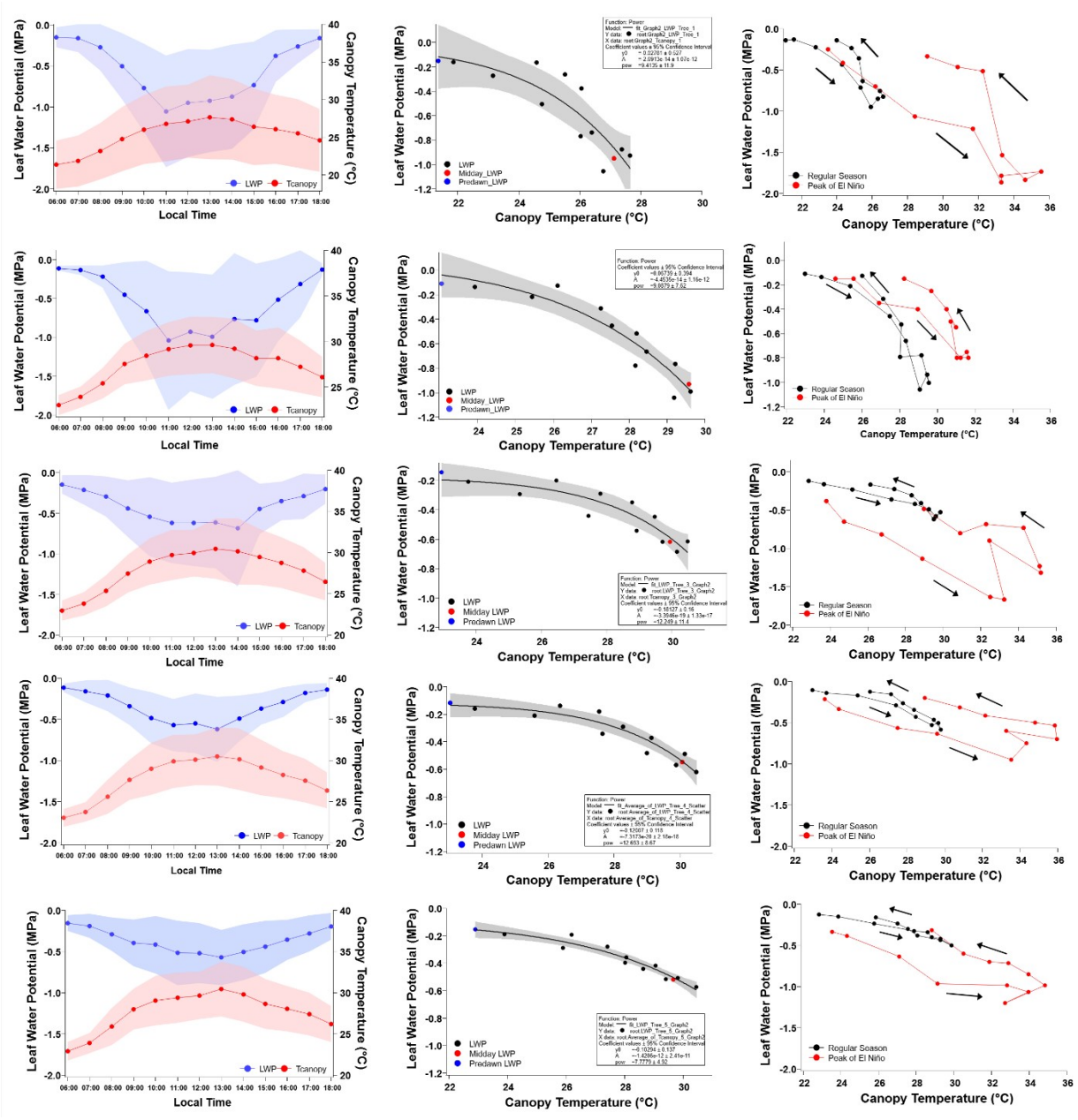


Figure 4 - Simulations of the hysteresis phenomenon and the size of the loop due to the absence of temporal and spatial difference between the stomatal conductance peak (g_s) and the peak of the vapor pressure deficit (VPD); (**A**) absence of temporal and spatial difference; (**B, C, D**) presence of only temporal difference; (**E**) presence of spatial difference only; (**F, G, H**) presence of spatial and temporal differences. In this figure it is possible to observe that only the temporal difference (**B, C, D**) is responsible for the appearance and size of the hysteresis loop between V_s and VPD , while the effect of the spatial difference (magnitude of the difference between g_s and VPD on the y axis) has no effect on the appearance and size of the hysteresis loop

(RQ-3) Leaf water potential and canopy temperature



Missing interpretation of LWP x Tcanopy results.

Discussion

Stomatal conductance and vapor pressure deficit dependencies

Plants can alter stomatal pore aperture by actively adjusting guard cell turgor pressure, which moderates gas exchange rates between the leaf interior and the atmosphere depending on the environmental conditions (Bertolino et al., 2019). The stoma is the main pathway of gas exchange processes (Brodribb et al., 2020b), and stomatal conductance (g_s) is a measure of the “facility” in which these processes occurs (conductance is the opposite of resistance). One of the most important abiotic factors that affects stomatal conductance is temperature which is strictly related to VPD (Lloyd and Farquhar, 2008). Generally, stomatal conductance declines under high VPD and transpiration increases in most species up until a given VPD threshold (Grossiord et al., 2020). In these conditions, the loss of leaf turgor pressure results in a complete stomatal closure (Fontes et al., 2018; Sack et al., 2003).

The link between guard cell turgor and stomatal aperture provides a very efficient way to avoid hydraulic failure under high VPD (Brodribb et al., 2017). In the Amazon forest, VPD and temperature are narrowly correlated once the relative humidity is, in average, near 90% throughout the year (Kunert et al., 2017). The temperature effect on g_s is very similar to the VPD effect, and it can vary along the different portions of the crown due to light exposure (Rey-Sánchez et al., 2016). When VPD is low and stomata are fully open, temperature increases linearly with VPD (Grossiord et al., 2020). In this context, the temperature where g_s is optimal can be different for sun-exposed leaves in comparison to shade leaves and also between canopy and understory species (Kardiman and Ræbild, 2018; Tribuzy, 2005). In average, g_s was found to reach maximum values between 31–33°C, which is known as the optimum temperature for photosynthesis (T_{opt}), previously determined by (Slot and Winter, 2017) studying many tropical species in Panama.

During drought events such as El Niño-Southern Oscillation (ENSO) with high temperature, stomatal closure is the major factor responsible for photosynthesis reduction rates in

both upper canopy and understory trees (Santos et al., 2018). This observations are consistent with (Brodrribb et al., 2020b) statement: “*from reproduction to production, stomata are the master regulators*”. Nowadays, the challenge is to understand the dynamics of stomatal control between canopy and shade-adapted species of tropical ecosystems, as demonstrated by (Deans et al., 2019) which recent studies showed that understory temperate species possessed fast-opening but slow-closing stomata, consistent with ecological adaptation to maximize light fleck use. This tand it is prior for the climate models in 21st century (McDowell et al., 2019).

Hysteresis loops as a water stress indicator

In dry conditions trees close their stomata to avoid excessive water loss. During those periods the plant is metaphorically in a paradigm: closing the stomata prolongs its survival by reducing water loss, but at the same time decreases the capture of CO₂, which can result in higher risks of carbon starvation (McDowell et al., 2018). In addition, transpiration acts as a cooling mechanism for the leaves by lowering their temperature and protecting the tissues from oxidative stress (Drake et al., 2018; Jardine et al., 2015). In the Amazon forest, species have different strategies to control the excessive transpiration during increased *VPD*. One example of those mechanisms are the loss of leaves and the production of flowers (Borchert, 1994), which is associated with the increase of irradiance in the dry period (Huete et al., 2006). The process of loss of leaves and posteriorly leaf flushing in the beginning of dry period can decrease the transpiration rates as well as protection against parasites due the lower humidity (Lopes et al., 2016).

At leaf level transpiration rates (*E*) are dependent on *g_s* and *VPD* according to Fick's first law. Most of studies use the variables *VPD* and solar radiation to understand the dynamics of transpiration (*E*), evapotranspiration (*ET*) and stand sap flow (*SF*) due to the facilities to obtain those type of data, using sensors installed in flux towers and directly in the trees. The hysteresis phenomenon occurs when a given independent variable *x* does not cause the same response in a given variable *y*, when the variable *x* decreases (Zeppel et al., 2004). The temporal difference between the peak of *g_s* and the peak of *VPD* can be considered one of the main regulating factors of the observed hysteresis patterns in transpiration processes as demonstrated by this study (Figs

2, 3 and 4). In terms of ecophysiological studies hysteresis patterns are an important aspect to be considered in the current Earth System Models (ESMs) (Jasechko et al., 2013), especially during extreme drought events such as ENSO which is correlated with tree mortality in the Amazon forest (Aleixo et al., 2019).

In the Central Amazon, during the 2015-16 ENSO, it was found that the transpiration rates of some species decreased as the dry period extended (Fontes et al., 2018). In contrast, Brum et al., 2018 found higher transpiration rates, reflected in a higher H_{index} , in eastern Amazon, when the dry period was compared to the wet period in the same drought event. This contrasting observations can be explained by the different transpiration sensitiveness according to ecological status of the forest (e.g. secondary vs mature) (Bretfeld et al., 2018; Mallick et al., 2016a), the size of the trees (Rowland et al., 2015) and across different precipitation gradients (Grossiord et al., 2019). Also, the distinct floristic structure associated with the gradient of soil fertility from east (low fertility) to west (high fertility) with different turn-over rates in the Amazon basin are also one possible explanation for observed drought sensitivity between the eastern and central Amazon. Another possible explanation for the observed higher transpiration H_{index} during 2015-16 ENSO in the eastern Amazon is the presence of deep roots (Nepstad et al., 1994) combined with hydraulic redistribution, which maintains the availability of water even during drought conditions (Oliveira et al., 2005). It seems that despite the extremely dry conditions the soil still have enough moisture to supply the trees enabling the stomata to be opening and avoiding transpiration threshold resulting in a hydraulic failure.

The magnitude of hysteresis depends strictly on the time lag between VPD, g_s and radiation, while soil moisture regulates these relationships (Bretfeld et al., 2018; Zheng et al., 2014). Using the Fick's first law (transpiration = $g_s \times VPD$), computational simulations demonstrated that temporal changes between g_s and VPD strongly alter transpiration H_{index} , as same as the spatial difference between these variables (**Fig. 3**). The greater temporal amplitude (TA_x) between the peaks of g_s and VPD, the greater will be the H_{index} . Conversely, contrasting the numeral amplitudes (Na_y) between g_s and VPD, together with the temporal amplitude, does not imply in a higher H_{index} in comparison to the effects of temporal amplitude alone (**Figs 2, 3**). These simulations imply that higher VPDs with a strong stomatal control does not cause a higher transpiration rates reflected in a higher H_{index} .

In this study, counterclockwise relationship between transpiration and VPD was observed, which can be explained due to the greater stomatal response to VPD and lower leaf water potential during the afternoon (Zeppel et al., 2004). This behavior is observed by several authors in different ecosystems (Bretfeld et al., 2018; Brum et al., 2018; Gimenez et al., 2019; Mallick et al., 2016; Zheng et al., 2014). The Hysteresis phenomena allow to infer about the biotic and abiotic factors that limit transpiration (Bretfeld et al., 2018; Mallick et al., 2016b; Zheng et al., 2014) and also makes it possible to infer about how extreme drought events can affect forest transpiration at different scales (Bretfeld et al., 2018; Brum et al., 2018; Christoffersen et al., 2016). Thus, the H_{index} from a large number of species is a good way of constraining ranges of hysteresis effects comparing, for example, drought events with normal periods on the same site, and using, when it is possible, the same trees. This kind of approach is highly important to understand the transpiration dynamics and the water use efficiency of the trees in a changing climate (Hatfield and Dold, 2019), especially in tropical ecosystems with their high diversity and different range of functional traits (McDowell et al., 2018).

Leaf water potential and atmospheric demand

In places on the globe where temperatures are suitable for plant development, the occurrence of trees is mainly controlled by the water supply, which is essential for the growth and formation of new tissues (Meinzer, et al., 2004). The existence of trees only became possible after the development of a vascular system that allowed a continuous movement of water, in the order of $1\text{-}5\text{ m h}^{-1}$ with a low energy cost (Granier 1986). Even with an efficient water conduction system, it is only after a few days that the water contained in the soil reaches the top of a tree (Goldstein et al., 1998). One way for plants to minimize this delay is to use the water stored in tissues with high evaporative demand such as trunk, leaves and branches, which is known as capacitance (Goldstein et al., 1998; Meinzer, et al., 2004). Capacitance can be defined as the ratio of change in water content to change in water potential of a tissue and it was being formally incorporated into Own's law analogue to models that describe water transport along the soil-plant-atmosphere continuum (Meinzer et al., 2004, Cowan 1972, Philips et al., 1997).

The differences between water loss and uptake form a pressure gradient from roots to leaves, being the driving force for water movement in plants (Wheeler and Stroock 2008). This

pressure gradient can be measured by leaf water potential (Ψ_L) experiments where: values close to zero means little water loss (low potential gradient between soil and leaves) and more negative Ψ_L values mean high water loss (high potential gradient between soil and leaves) (Jarvis 1976; Hölttä and Sperry 2014). The water moves from a high-water potential level to lower water potential level in a process described by cohesion-tension theory (Dixon e Joly, 1894). In this context, canopy trees are generally under higher evaporative demand conditions which require more extensive and in-deep root systems to guarantee their physical stability, which reflects higher soil volumes to access water (Oliveira et al., 2005).

In the central Amazon, species from plateaus are more adaptable to drought conditions, and, therefore, invests in higher hydraulic safety with higher wood density, lower mean vessel hydraulic diameter, lower mean vessel area and smaller stem cross-sectional sapwood area than species in valley (Cosme et al., 2017). These functional traits of plateau species are associated with isohydric characteristics where the stomata act to prevent Ψ_L from dropping below a critical threshold level (Fisher et al., 2006). Although Ψ_L did not significantly improve prediction of g_s in tropical canopy trees (Wu et al., 2020), stomatal sensitivity to Ψ_L strong relates to xylem characteristics (Klein, 2014). The hydraulic resistance of leaves such as Ψ_L can be highly variable over short time scales, uncoupling tension in the xylem of leaves from that in the stems to which they are attached (Meinzer et al., 2008), and it is the possible explanation to difficulty to incorporate Ψ_L in g_s models. Another important aspect to consider is the mechanism of foliar water uptake (FU) which is a significant process in determining how forests interact with climate, and could alter our interpretation of current metrics for hydraulic stress and sensitivity (Binks et al., 2019).

On the other hand, diurnal responses of Ψ_L to temperature are more significant and predictable. The leaf surface of canopy trees can be considered the last layer of the soil-plant-atmosphere continuum. Changes in Ψ_L are related to changes in temperature and soil moisture. In this perspective, canopy temperature (T_{canopy}) is a good proxy for daily and seasonal Ψ_L variations. During the sunnier dry season in the Amazon reflected in higher temperature rates (Huete et al., 2006), plants can sustain low Ψ_L for a substantial amount of time and still recover after a re-hydration period due to the passage of clouds or occasional rains (Fontes et al., 2018).

The nonlinear relationship between Ψ_L and T_{canopy} observed by this study (Fig XX) is similar to the relationship between Ψ_L and soil moisture described by (Carroll et al., 2019), attesting the pressure gradient coupling of soil-plant-atmosphere continuum.

Conclusion

Acknowledgments

This material is based upon work supported as part of the Next Generation Ecosystem Experiments-Tropics (NGEE-Tropics), as part of DOE's Terrestrial Ecosystem Science Program – Contract No. DE-AC02-05CH11231. Additional funding for this research was provided by the Coordenação de Aperfeiçoamento de Pessoal de Nível Superior (CAPES). The authors are thankful to the logistical and scientific support provided by the Laboratório de Manejo Florestal (LMF) and the Large-Scale Biosphere-Atmosphere Program (LBA) at the National Institute of Amazonian Research (INPA).

References

- Aleixo, I., Norris, D., Hemerik, L., Barbosa, A., Prata, E., Costa, F., Poorter, L., 2019. Amazonian rainforest tree mortality driven by climate and functional traits. *Nat. Clim. Chang.* 9, 384.
- Aparecido, L.M.T., Dos Santos, J., Higuchi, N., Kunert, N., 2019. Relevance of wood anatomy and size of amazonian trees in the determination and allometry of sapwood area. *Acta Amaz.* 49, 1–10. <https://doi.org/10.1590/1809-4392201800961>
- Araújo, A.C., Nobre, A.D., Kruijt, B., Elbers, J.A., Dallarosa, R., Stefani, P., von Randow, C., Manzi, A.O., Culf, A.D., Gash, J.H.C., Valentini, R., Kabat, P., 2002. Comparative measurements of carbon dioxide fluxes from two nearby towers in a central Amazonian

- rainforest: The Manaus LBA site. *J. Geophys. Res.* 107, 8090. <https://doi.org/10.1029/2001JD000676>
- Bertolino, L.T., Caine, R.S., Gray, J.E., 2019. Impact of Stomatal Density and Morphology on Water-Use Efficiency in a Changing World. *Front. Plant Sci.*
- Binks, O., Meir, P., Rowland, L., da Costa, A.C.L., Vasconcelos, S.S., de Oliveira, A.A.R., Ferreira, L., Christoffersen, B., Nardini, A., Mencuccini, M., 2016. Plasticity in leaf-level water relations of tropical rainforest trees in response to experimental drought. *New Phytol.* 211, 477–488.
- Binks, O., Mencuccini, M., Rowland, L., da Costa, A.C.L., de Carvalho, C.J.R., Bittencourt, P., Eller, C., Teodoro, G.S., Carvalho, E.J.M., Soza, A., 2019. Foliar water uptake in Amazonian trees: Evidence and consequences. *Glob. Chang. Biol.* 25, 2678–2690.
- Borchert, R., 1994. Soil and stem water storage determine phenology and distribution of tropical dry forest trees. *Ecology* 75, 1437–1449.
- Braden, B., 1986. The surveyor's area formula. *Coll. Math. J.* 17, 326–337.
- Bretfeld, M., Ewers, B.E., Hall, J.S., 2018. Plant water use responses along secondary forest succession during the 2015–2016 El Niño drought in Panama. *New Phytol.* 219, 885–899.
- Brodribb, T.J., McAdam, S.A.M., Carins Murphy, M.R., 2017. Xylem and stomata, coordinated through time and space. *Plant. Cell Environ.* 40, 872–880.
- Brodribb, T.J., Powers, J., Cochard, H., Choat, B., 2020a. Hanging by a thread? Forests and drought. *Science* (80-.). 368, 261–266.
- Brodribb, T.J., Sussmilch, F., McAdam, S.A.M., 2020b. From reproduction to production, stomata are the master regulators. *Plant J.* 101, 756–767.
- Brum, M., Gutiérrez López, J., Asbjornsen, H., Licata, J., Pypker, T., Sanchez, G., Oiveira, R.S., 2018. ENSO effects on the transpiration of eastern Amazon trees. *Philos. Trans. R. Soc. B Biol. Sci.* 373, 20180085.
- Burgess, S.S.O., Adams, M.A., Turner, N.C., Beverly, C.R., Ong, C.K., Khan, A.A.H., Bleby, T.M., 2001. An improved heat pulse method to measure low and reverse rates of sap flow in woody plants. *Tree Physiol.* 21, 589–598.
- Cardoso, D., Särkinen, T., Alexander, S., Amorim, A.M., Bittrich, V., Celis, M., Daly, D.C., Fiaschi, P., Funk, V.A., Giacomini, L.L., Goldenberg, R., Heiden, G., Iganci, J., Kelloff, C.L., Knapp, S., Cavalcante de Lima, H., Machado, A.F.P., dos Santos, R.M., Mello-Silva, R., Michelangeli, F.A., Mitchell, J., Moonlight, P., de Moraes, P.L.R., Mori, S.A., Nunes, T.S., Pennington, T.D., Pirani, J.R., Prance, G.T., de Queiroz, L.P., Rapini, A., Riina, R., Rincon, C.A.V., Roque, N., Shimizu, G., Sobral, M., Stehmann, J.R., Stevens, W.D., Taylor, C.M., Trovó, M., van den Berg, C., van der Werff, H., Viana, P.L., Zartman, C.E., Forzza, R.C., 2017. Amazon plant diversity revealed by a taxonomically verified species list. *Proc. Natl. Acad. Sci.* 114, 10695 LP – 10700. <https://doi.org/10.1073/pnas.1706756114>
- Carroll, C.J.W., Martin, P.H., Knapp, A.K., Ocheltree, T.W., 2019. Temperature induced shifts in leaf water relations and growth efficiency indicate climate change may limit aspen growth in the Colorado Rockies. *Environ. Exp. Bot.* 159, 132–137.
- Chambers, J.Q., Artaxo, P., 2017. Biosphere-atmosphere interactions: Deforestation size influences rainfall. *Nat. Clim. Chang.* 7, 175.
- Christianson, D.S., Varadharajan, C., Christoffersen, B., Detto, M., Faybishenko, B., Gimenez, B.O., Hendrix, V., Jardine, K.J., Negron-Juarez, R., Pastorello, G.Z., Powell, T.L., Sandesh, M., Warren, J.M., Wolfe, B.T., Chambers, J.Q., Kueppers, L.M., McDowell, N.G., Agarwal, D.A., 2017. A metadata reporting framework (FRAMES) for synthesis of ecohydrological observations. *Ecol. Inform.* 42. <https://doi.org/10.1016/j.ecoinf.2017.06.002>
- Christoffersen, B.O., Gloor, M., Fauset, S., Fyllas, N.M., Galbraith, D.R., Baker, T.R., Kruijt, B., Rowland, L., Fisher, R.A., Binks, O.J., Sevanto, S., Xu, C., Jansen, S., Choat, B., Mencuccini, M., McDowell, N.G., Meir, P., 2016. Linking hydraulic traits to tropical forest function in a size-structured and trait-driven model (TFS v.1-Hydro). *Geosci. Model Dev.* 9, 4227–4255. <https://doi.org/10.5194/gmd-9-4227-2016>
- Cosme, L.H.M., Schiatti, J., Costa, F.R.C., Oliveira, R.S., 2017. The importance of hydraulic architecture to the distribution patterns of trees in a central Amazonian forest. *New*

- Phytol. 215, 113–125. <https://doi.org/10.1111/nph.14508>
- Cowan, I.R., Farquhar, G.D., 1977. Stomatal function in relation to leaf metabolism and environment., in: *Symposia of the Society for Experimental Biology*. p. 471.
- Deans, R.M., Brodribb, T.J., Busch, F.A., Farquhar, G.D., 2019. Plant water-use strategy mediates stomatal effects on the light induction of photosynthesis. *New Phytol.* 222, 382–395.
- Drake, J.E., Tjoelker, M.G., Vårhammar, A., Medlyn, B.E., Reich, P.B., Leigh, A., Pfautsch, S., Blackman, C.J., López, R., Aspinwall, M.J., 2018. Trees tolerate an extreme heatwave via sustained transpirational cooling and increased leaf thermal tolerance. *Glob. Chang. Biol.* 24, 2390–2402.
- Eltahir, E.A.B., Bras, R.L., 1994. Precipitation recycling in the Amazon basin. *Q. J. R. Meteorol. Soc.* 120, 861–880. <https://doi.org/10.1002/qj.49712051806>
- Farquhar, G.D., von Caemmerer, S. von, Berry, J.A., 1980. A biochemical model of photosynthetic CO₂ assimilation in leaves of C₃ species. *Planta* 149, 78–90.
- Fisher, R.A., Williams, M., Do Vale, R.L., Da Costa, A.L., Meir, P., 2006. Evidence from Amazonian forests is consistent with isohydric control of leaf water potential. *Plant. Cell Environ.* 29, 151–165.
- Fontes, C.G., Dawson, T.E., Jardine, K., McDowell, N., Gimenez, B.O., Anderegg, L., Negrón-Juárez, R., Higuchi, N., Fine, P.V.A., Araújo, A.C., 2018. Dry and hot: the hydraulic consequences of a climate change-type drought for Amazonian trees. *Philos. Trans. R. Soc. B Biol. Sci.* 373, 20180209.
- Giardina, F., Konings, A.G., Kennedy, D., Alemohammad, S.H., Oliveira, R.S., Uriarte, M., Gentine, P., 2018. Tall Amazonian forests are less sensitive to precipitation variability. *Nat. Geosci.* 11, 405–409.
- Gimenez, B.O., Jardine, K.J., Higuchi, N., Negrón-Juárez, R.I., Sampaio-Filho, I. de J., Cobello, L.O., Fontes, C.G., Dawson, T.E., Varadharajan, C., Christianson, D.S., Spanner, G.C., Araújo, A.C., Warren, J.M., Newman, B.D., Holm, J.A., Koven, C.D., McDowell, N.G., Chambers, J.Q., 2019. Species-specific shifts in diurnal sap velocity dynamics and hysteretic behavior of ecophysiological variables during the 2015–2016 el niño event in the amazon forest. *Front. Plant Sci.* 10, 1–16. <https://doi.org/10.3389/fpls.2019.00830>
- Green, S., Clothier, B., Jardine, B., 2003. Theory and practical application of heat pulse to measure sap flow. *Agron. J.* 95, 1371–1379.
- Grossiord, C., Buckley, T.N., Cernusak, L.A., Novick, K.A., Poulter, B., Siegwolf, R.T.W., Sperry, J.S., McDowell, N.G., 2020. Plant responses to rising vapor pressure deficit. *New Phytol.*
- Grossiord, C., Christoffersen, B., Alonso-Rodríguez, A.M., Anderson-Teixeira, K., Asbjornsen, H., Aparecido, L.M.T., Carter Berry, Z., Baraloto, C., Bonal, D., Borrego, I., Burban, B., Chambers, J.Q., Christianson, D.S., Detto, M., Faybishenko, B., Fontes, C.G., Fortunel, C., Gimenez, B.O., Jardine, K.J., Kueppers, L., Miller, G.R., Moore, G.W., Negron-Juarez, R., Stahl, C., Swenson, N.G., Trotsiuk, V., Varadharajan, C., Warren, J.M., Wolfe, B.T., Wei, L., Wood, T.E., Xu, C., McDowell, N.G., 2019. Precipitation mediates sap flux sensitivity to evaporative demand in the neotropics. *Oecologia*. <https://doi.org/10.1007/s00442-019-04513-x>
- Hatfield, J.L., Dold, C., 2019. Water-Use Efficiency: Advances and Challenges in a Changing Climate . *Front. Plant Sci.* .
- Higuchi, N., Suwa, R., Higuchi, F.G., Lima, A.J.N., dos Santos, J., Noguchi, H., Kajimoto, T., Ishizuka, M., 2016. Overview of Forest Carbon Stocks Study in Amazonas State, Brazil BT - Interactions Between Biosphere, Atmosphere and Human Land Use in the Amazon Basin, in: Nagy, L., Forsberg, B.R., Artaxo, P. (Eds.), . Springer Berlin Heidelberg, Berlin, Heidelberg, pp. 171–187. https://doi.org/10.1007/978-3-662-49902-3_9
- Huete, A.R., Didan, K., Shimabukuro, Y.E., Ratana, P., Saleska, S.R., Hutyrá, L.R., Yang, W., Nemani, R.R., Myneni, R., 2006. Amazon rainforests green-up with sunlight in dry season. *Geophys. Res. Lett.* 33.
- Jardine, K.J., Chambers, J.Q., Holm, J., Jardine, A.B., Fontes, C.G., Zorzanelli, R.F., Meyers, K.T., de Souza, V.F., Garcia, S., Gimenez, B.O., Piva, L.R. de O., Higuchi, N., Artaxo, P.,

- Martin, S., Manzi, A.O., 2015. Green Leaf Volatile Emissions during High Temperature and Drought Stress in a Central Amazon Rainforest. *Plants* 4, 678–690. <https://doi.org/10.3390/plants4030678>
- Jasechko, S., Sharp, Z.D., Gibson, J.J., Birks, S.J., Yi, Y., Fawcett, P.J., 2013. Terrestrial water fluxes dominated by transpiration. *Nature* 496, 347–350.
- Kardiman, R., Ræbild, A., 2018. Relationship between stomatal density, size and speed of opening in Sumatran rainforest species. *Tree Physiol.* 38, 696–705.
- Klein, T., 2014. The variability of stomatal sensitivity to leaf water potential across tree species indicates a continuum between isohydric and anisohydric behaviours. *Funct. Ecol.* 28, 1313–1320.
- Kunert, N., Aparecido, L.M.T., Wolff, S., Higuchi, N., Santos, J. dos, Araujo, A.C. de, Trumbore, S., 2017. A revised hydrological model for the Central Amazon: The importance of emergent canopy trees in the forest water budget. *Agric. For. Meteorol.* 239, 47–57. <https://doi.org/10.1016/j.agrformet.2017.03.002>
- Lambers, H., Chapin III, F.S., Pons, T.L., 2008. *Plant physiological ecology*. Springer Science & Business Media.
- Lloyd, J., Farquhar, G.D., 2008. Effects of rising temperatures and [CO₂] on the physiology of tropical forest trees. *Philos. Trans. R. Soc. B Biol. Sci.* 363, 1811–1817. <https://doi.org/10.1098/rstb.2007.0032>
- Lopes, A.P., Nelson, B.W., Wu, J., de Alencastro Graça, P.M.L., Tavares, J.V., Prohaska, N., Martins, G.A., Saleska, S.R., 2016. Leaf flush drives dry season green-up of the Central Amazon. *Remote Sens. Environ.* 182, 90–98.
- Lugli, L.F., Andersen, K.M., Aragão, L.E.O.C., Cordeiro, A.L., Cunha, H.F. V, Fuchslueger, L., Meir, P., Mercado, L.M., Oblitas, E., Quesada, C.A., Rosa, J.S., Schaap, K.J., Valverde-Barrantes, O., Hartley, I.P., 2019. Multiple phosphorus acquisition strategies adopted by fine roots in low-fertility soils in Central Amazonia. *Plant Soil*. <https://doi.org/10.1007/s11104-019-03963-9>
- Mallick, K., Trebs, I., Boegh, E., Giustarini, L., Schlerf, M., Drewry, D.T., Hoffmann, L., RANDOW, C. von, Kruijt, B., Araujo, A., 2016a. Canopy-scale biophysical controls of transpiration and evaporation in the Amazon Basin. *Embrapa Amaz. Orient. em periódico indexado*.
- Mallick, K., Trebs, I., Boegh, E., Giustarini, L., Schlerf, M., Drewry, D.T., Hoffmann, L., Von Randow, C., Kruijt, B., Araujo, A., Saleska, S., Ehleringer, J.R., Domingues, T.F., Ometto, J.P.H.B., Nobre, A.D., Luiz Leal De Moraes, O., Hayek, M., William Munger, J., Wofsy, S.C., 2016b. Canopy-scale biophysical controls of transpiration and evaporation in the Amazon Basin. *Hydrol. Earth Syst. Sci.* 20, 4237–4264. <https://doi.org/10.5194/hess-20-4237-2016>
- McDowell, N., Allen, C.D., Anderson-Teixeira, K., Brando, P., Brienen, R., Chambers, J., Christoffersen, B., Davies, S., Doughty, C., Duque, A., Espirito-Santo, F., Fisher, R., Fontes, C.G., Galbraith, D., Goodsman, D., Grossiord, C., Hartmann, H., Holm, J., Johnson, D.J., Kassim, A.R., Keller, M., Koven, C., Kueppers, L., Kumagai, T., Malhi, Y., McMahon, S.M., Mencuccini, M., Meir, P., Moorcroft, P., Muller-Landau, H.C., Phillips, O.L., Powell, T., Sierra, C.A., Sperry, J., Warren, J., Xu, C., Xu, X., 2018. Drivers and mechanisms of tree mortality in moist tropical forests. *New Phytol.* 219, 851–869. <https://doi.org/10.1111/nph.15027>
- McDowell, N.G., Brodrigg, T.J., Nardini, A., 2019. Hydraulics in the 21 st century . *New Phytol.* 224, 537–542. <https://doi.org/10.1111/nph.16151>
- Meinzer, F.C., Woodruff, D.R., Domec, J.-C., Goldstein, G., Campanello, P.I., Gatti, M.G., Villalobos-Vega, R., 2008. Coordination of leaf and stem water transport properties in tropical forest trees. *Oecologia* 156, 31–41.
- Nepstad, D.C., de Carvalho, C.R., Davidson, E.A., Jipp, P.H., Lefebvre, P.A., Negreiros, G.H., da Silva, E.D., Stone, T.A., Trumbore, S.E., Vieira, S., 1994. The role of deep roots in the hydrological and carbon cycles of Amazonian forests and pastures. *Nature* 372, 666–669.
- O'Brien, J.J., Oberbauer, S.F., Clark, D.B., 2004. Whole tree xylem sap flow responses to

- multiple environmental variables in a wet tropical forest. *Plant. Cell Environ.* 27, 551–567.
- Oliveira, R.S., Dawson, T.E., Burgess, S.S.O., Nepstad, D.C., 2005. Hydraulic redistribution in three Amazonian trees. *Oecologia* 145, 354–363.
- Rey-Sánchez, A.C., Slot, M., Posada, J.M., Kitajima, K., 2016. Spatial and seasonal variation in leaf temperature within the canopy of a tropical forest. *Clim. Res.* 71, 75–89.
- Rowland, L., da Costa, A.C.L., Galbraith, D.R., Oliveira, R.S., Binks, O.J., Oliveira, A.A.R., Pullen, A.M., Doughty, C.E., Metcalfe, D.B., Vasconcelos, S.S., 2015. Death from drought in tropical forests is triggered by hydraulics not carbon starvation. *Nature* 528, 119–122.
- Sack, L., Cowan, P.D., Jaikumar, N., Holbrook, N.M., 2003. The ‘hydrology’ of leaves: coordination of structure and function in temperate woody species. *Plant. Cell Environ.* 26, 1343–1356.
- Salati, E., Vose, P.B., 1984. Amazon basin: a system in equilibrium. *Science* (80-.). 225, 129–138.
- Sampaio Filho, D.I., Jardine, J.K., De Oliveira, C.R., Gimenez, O.B., Cobello, O.L., Piva, R.L., Candido, A.L., Higuchi, N., Chambers, Q.J., 2018. Below versus above Ground Plant Sources of Abscisic Acid (ABA) at the Heart of Tropical Forest Response to Warming. *Int. J. Mol. Sci.* . <https://doi.org/10.3390/ijms19072023>
- Santos, V.A.H.F. dos, Ferreira, M.J., Rodrigues, J.V.F.C., Garcia, M.N., Ceron, J.V.B., Nelson, B.W., Saleska, S.R., 2018. Causes of reduced leaf-level photosynthesis during strong El Niño drought in a Central Amazon forest. *Glob. Chang. Biol.* 24, 4266–4279.
- Slot, M., Winter, K., 2017. In situ temperature response of photosynthesis of 42 tree and liana species in the canopy of two Panamanian lowland tropical forests with contrasting rainfall regimes. *New Phytol.* 214, 1103–1117. <https://doi.org/10.1111/nph.14469>
- ter Steege, H., Pitman, N.C. a, Sabatier, D., Baraloto, C., Salomão, R.P., Guevara, J.E., Phillips, O.L., Castilho, C. V, Magnusson, W.E., Molino, J.-F., Monteagudo, A., Núñez Vargas, P., Montero, J.C., Feldpausch, T.R., Coronado, E.N.H., Killeen, T.J., Mostacedo, B., Vasquez, R., Assis, R.L., Terborgh, J., Wittmann, F., Andrade, A., Laurance, W.F., Laurance, S.G.W., Marimon, B.S., Marimon, B.-H., Guimarães Vieira, I.C., Amaral, I.L., Brienen, R., Castellanos, H., Cárdenas López, D., Duivenvoorden, J.F., Mogollón, H.F., Matos, F.D.D.A., Dávila, N., García-Villacorta, R., Stevenson Diaz, P.R., Costa, F., Emilio, T., Levis, C., Schiatti, J., Souza, P., Alonso, A., Dallmeier, F., Montoya, A.J.D., Fernandez Piedade, M.T., Araujo-Murakami, A., Arroyo, L., Gribel, R., Fine, P.V. a, Peres, C. a, Toledo, M., Aymard C, G. a, Baker, T.R., Cerón, C., Engel, J., Henkel, T.W., Maas, P., Petronelli, P., Stropp, J., Zartman, C.E., Daly, D., Neill, D., Silveira, M., Paredes, M.R., Chave, J., Lima Filho, D.D.A., Jørgensen, P.M., Fuentes, A., Schöngart, J., Cornejo Valverde, F., Di Fiore, A., Jimenez, E.M., Peñuela Mora, M.C., Phillips, J.F., Rivas, G., van Andel, T.R., von Hildebrand, P., Hoffman, B., Zent, E.L., Malhi, Y., Prieto, A., Rudas, A., Ruschell, A.R., Silva, N., Vos, V., Zent, S., Oliveira, A. a, Schutz, A.C., Gonzales, T., Trindade Nascimento, M., Ramirez-Angulo, H., Sierra, R., Tirado, M., Umaña Medina, M.N., van der Heijden, G., Vela, C.I. a, Vilanova Torre, E., Vriesendorp, C., Wang, O., Young, K.R., Baider, C., Balslev, H., Ferreira, C., Mesones, I., Torres-Lezama, A., Urrego Giraldo, L.E., Zagt, R., Alexiades, M.N., Hernandez, L., Huamantupa-Chuquimaco, I., Milliken, W., Palacios Cuenca, W., Pauletto, D., Valderrama Sandoval, E., Valenzuela Gamarra, L., Dexter, K.G., Feeley, K., Lopez-Gonzalez, G., Silman, M.R., 2013. Hyperdominance in the Amazonian tree flora. *Science* 342, 1243092.
- Tribuzy, E.S., 2005. Variações da temperatura foliar do dossel e o seu efeito na taxa assimilatória de CO₂ na Amazônia Central.
- Woo, K.B., Boersma, L., Stone, L.N., 1966. Dynamic simulation model of the transpiration process. *Water Resour. Res.* 2, 85–97. <https://doi.org/10.1029/WR002i001p00085>
- Wu, J., Serbin, S.P., Ely, K.S., Wolfe, B.T., Dickman, L.T., Grossiord, C., Michaletz, S.T., Collins, A.D., Detto, M., McDowell, N.G., 2020. The response of stomatal conductance to seasonal drought in tropical forests. *Glob. Chang. Biol.* 26, 823–839.
- Zeppel, M.J.B., Murray, B.R., Barton, C., Eamus, D., 2004. Seasonal responses of xylem sap

- velocity to VPD and solar radiation during drought in a stand of native trees in temperate Australia. *Funct. Plant Biol.* 31, 461–470.
- Zheng, H., Wang, Q., Zhu, X., Li, Y., Yu, G., 2014. Hysteresis responses of evapotranspiration to meteorological factors at a diel timescale: Patterns and causes. *PLoS One* 9, 1–10. <https://doi.org/10.1371/journal.pone.0098857>
- Zuecco, G., Penna, D., Borga, M., van Meerveld, H.J., 2016. A versatile index to characterize hysteresis between hydrological variables at the runoff event timescale. *Hydrol. Process.* 30, 1449–1466.